

# EVALUATION OF HEAT TRANSFER CORRELATIONS FOR HELICAL COILS BASED ON MEASUREMENTS OF A SOLAR ORC OPERATING AT SUBCRITICAL CONDITIONS

Kaya A.,\*<sup>1</sup> Lazova M<sup>1</sup>, Kosmadakis G<sup>2</sup> and De Paepe M.<sup>1</sup>

\*Author for correspondence

<sup>1</sup>Department of Flow, Heat and Combustion Mechanics,  
Ghent University,  
Ghent, 9000,  
Belgium,

E-mail: [alihan.kaya@ugent.be](mailto:alihan.kaya@ugent.be)

<sup>2</sup>Department of Natural Resources & Agricultural Engineering,  
Agricultural University of Athens,  
Athens, Greece

## ABSTRACT

Organic Rankine cycle (ORC) is an acknowledged method for utilizing low temperature heat sources for generating electricity. Among many applications at heat sources such as internal combustion engines and industrial facilities, solar power is a significant energy source. For solar boilers, helical coil heat exchangers are widely used. The design of these heat exchangers are made with conventional methods, which are mostly not validated for ORC conditions, namely larger tube diameters and working fluids. In order to analyse the accuracy of conventional helical coil heat transfer correlations in design, the geometry and performed measurements at subcritical conditions of a helical coil heat exchanger is taken as reference for the off-design. The helical coil is electrically heated for simulating the photovoltaic/thermal (PV/T) collectors, for testing the solar ORC concept. Then the ORC is coupled with the PV/T collectors on the field for the complete solar ORC system. The inlet conditions of the existing installation are used for sizing and rating via 9 two-phase heat transfer correlations existing in the literature for the tube-side of helical coil. The helical coil outer diameter is 33,7 mm, whereas the shell inner and outer diameter are 0,526 m and 0,674 m, respectively. The coil diameter is 0,6 m. Three measurements are made at changing ORC medium (R404a) mass flow rates, namely 0,1 kg/s, 0,17 kg/s and 0,24 kg/s. R404a's inlet temperature changes between 21,9 °C and 33,6 °C at a pressure range of 17,5 – 31,6 bars (representing the saturation temperature). In all three cases, the heating water inlet conditions are fixed at an inlet temperature of 95,3 °C and a mass flow rate of 2,67 kg/s.

## INTRODUCTION

The increasing concerns over world's energy shortage lead researchers to investigate sustainable methods for energy production. In the last decades, Organic Rankine cycle (ORC) is a thermodynamic cycle which has become a popular method for producing electricity (magnitudes of both MWs and kW) by means of utilizing various heat sources. The Organic Rankine Cycle and the conventional Steam Rankine Cycle are similar thermodynamic concepts. ORCs are composed of four

main components, namely an evaporator, a condenser, a pump and an expansion unit (turbine or expander). The distinguishing feature of ORCs is the fact that ORCs utilize low Global Warming Potential (GWP) and Ozone Depletion Potential (ODP) organic working fluids instead of water. Organic fluids have low boiling points, which lead to evaporation in much lower temperatures in comparison to water. Hence, heat sources down to 60°C can be utilized for electricity generation. Common heat sources are biomass, geothermal, solar and waste heat resulting from industrial processes or internal combustion engines. Usually, available heat to be utilized is divided into two main groups as low-temperature (<250°C) and high-temperature (>250°C) heat sources.

## NOMENCLATURE

$D, d$	[m]	Diameter
$h$	[W/m <sup>2</sup> K]	Convective heat transfer coefficient
$L$	[m]	Length
$\dot{m}$	[kg/s]	Mass flowrate
$P$	[Pa]	Pressure
$p$	[m]	Helical tube pitch
$Q$	[W]	Transferred heat
$T$	[°C]	Temperature
$x$	[-]	Vapour quality

### Subscripts

$av$	Average
$c$	Coil
$cf$	Cold fluid
$dev$	Deviation
$hf$	Hot fluid
$i$	Discretisation step
$in$	Inlet
$o$	Outlet
$ph$	Preheating
$t$	Tube (Bare)
$sat$	Saturation
$sh$	Superheating
$tp$	Two phase
$w$	Tube wall

In ORCs, the high pressure organic liquid is evaporated and subsequently expanded for mechanical work release. Then the

low pressure vapour is condensed and pumped further to the evaporator via a pump as high pressure liquid. The evaporator is where the heat is transferred from an external (or an intermediate heat carrier loop) heat source to the working fluid. There are various research available regarding ORCs and can be divided into three main concepts as cycle level, working fluid selection and component level research. Cycle level research focuses on the improvement and optimization of the cycle's thermo-economic optimization [1]. The working fluid selection research is mainly related to the analysis of the working fluids' category (e.g. environmental properties), and the effect of their thermodynamic and physical properties on the ORC performance, within the frame of international environmental treaties like Kyoto and Montreal Protocols. In their study, Bao and Zhao provide an extensive review related to that topic [2]. Moreover, the component level research is mainly related to turbine (or expander) [2-3] and heat exchanger design [4-6].

It is reported in the literature that the heat exchangers (evaporator and condenser) may constitute a significant part (up to the half) of the investment cost of an ORC system [7-8]. Hence, the accuracy of the heat exchanger design becomes a crucial issue to investigate. Normally, the sizing of a helical coil heat exchanger is done by heat transfer correlations available in the literature. Although the literature on heat exchanger research in general is in a developed phase, research focusing on specific ORC cases (different geometries, temperatures and especially working fluids) is still at its infancy. In other words, these design methods are not necessarily validated for ORCs, and thus, might lead to unreliable designs or be prone to large errors. In addition to that, research related to two-phase flow heat transfer in helical coils is limited [9]. Thus, the helical coil evaporators for ORCs remain uninvestigated.

On the other hand, the wide application range of ORCs makes it combinable with different sustainable energy production methods, such as solar and geothermal systems. Due to the fact that ORCs are promising systems with good thermodynamic efficiency and lower investment cost, small scale applications (kW levels) are desirable. In parallel to that, concentrating solar power is a practiced and proven renewable energy method for converting sun's heat into electricity via ORCs [10-12]. Thus, the combination of these two phenomena is an interesting topic to investigate.

In accordance with the aforementioned research motivations, the study presents measurements performed on a new system for investigating the combination of Concentrated Photovoltaics/Thermal (CPV/T) and ORCs is built in Athens, Greece for experimental research. Moreover, the measurements results are taken as reference point for the off-design study of the helical coil heat exchanger, for assessing the prediction capability of 9 helical coil two-phase heat transfer correlations for ORCs with helical coils, whereas the single-phase heat transfer inside the helical coils and at the shell are calculated with a fixed method for comparison purposes.

## HEAT EXCHANGER AND MEASUREMENTS

A large range of measurements are done on the present helical coil and CPV/T system, even at supercritical conditions [13]. However only the measurements from subcritical ranges fall within the scope of this study, due to the fact that it involves the analysis of two-phase region inside helical coils.

The measurements are made at a helical coil tube of 66 m long, having an outer diameter of 33,7 mm (4 mm wall thickness), whereas the shell inner  $D_i$ , and outer diameter  $D_o$ , are 0,526 m and 0,674 m, respectively. The coil diameter  $D_c$  is 0,6 m. At the shell side (i.e. annulus) the heating water flows from the top to the bottom, whereas the ORC medium R404a flows from bottom toward the top. The R404a mass flow rate is changed to three values, namely 0,1 kg/s, 0,17 kg/s and 0,24 kg/s. In parallel to that change, R404a's inlet temperature changes between 21,9 °C and 33,6 °C at a pressure range of 17,5 – 31,6 bars (representing the saturation temperature). In all three cases, the heating water inlet conditions are fixed at an inlet temperature of 95,3 °C and a mass flow rate of 2,67 kg/s. The mentioned geometric parameters and flow directions regarding the helical coil evaporator are illustrated in Figure 1.

Temperatures are measured with PT100 type thermocouples, whereas the pressure is measured by pressure transmitters. The fluid properties are calculated via EES/Refprop database [14]. The mass flow rates at the shell and coil side are deduced from the measurements of temperature and pressure at the pump outlet, and the volume flow rate which is calculated via a linear correlation with pump speed in rpms. The transferred heat at the heat exchanger is then calculated via heat balance. The corresponding uncertainties of measurement devices and calculated parameters are listed in the Table 1. These values are in accordance with the previous study conducted by Kosmadakis et al. [15]. Moreover, the measured values that are to be used in this study are listed in the Table 2.

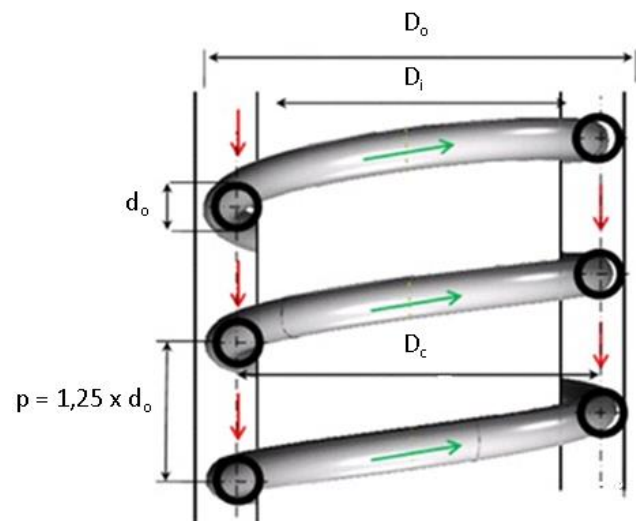


Figure 1 Helical coil evaporator

Table 1 Uncertainties in measurements

Measurement	Uncertainty	Units
Temperature, T	$\pm 0,2^{\circ}\text{C}$	$^{\circ}\text{C}$
Pressure, P	1 %	Pa

Mass flow rate, $\dot{m}$	2,33 %	kg/s
Thermodynamic Properties	1,2 %	
Transferred Heat, $Q$	2,62 %	W

**Table 2** Measurements

$\dot{m}_c$ [kg/s]	$P_{sat}$ [MPa]	$T_{sat}$ [°C]	$T_{ho}$ [°C]	$T_{co}$ [°C]	$Q$ [kW]
0,10	1,75	38,2	93,3	91,8	22,20
0,17	2,31	50	92,4	93,1	34,82
0,24	3,16	64,2	91,9	93,6	44,77

### OFF-DESIGN OF THE HELICAL COIL

In order to reveal the prediction capability of various two-phase helical coil heat transfer correlations, measurements on the existing ORC helical coil and the results of prediction methods are compared. The measured inlet and outlet temperatures of water (hot) and R404a (cold), total transferred heat, mass flow and the total coil length are taken as reference. The measured data from the experiment is taken as the boundary condition for designing via 9 correlations. The length predicted by each correlation is compared to the existing helical coil heat exchanger. A list of those correlations is given in the Table 3.

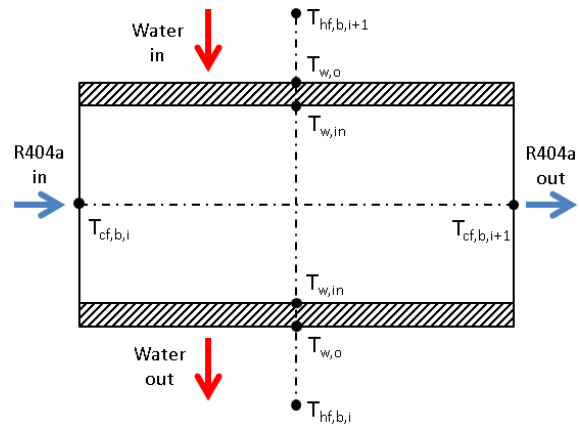
**Table 3** Heat transfer correlations for two-phase flow inside helical coils

Author(s)	Source
Campolunghi et al. (1975)	[16]
Chen (1966)	[17]
De La Harpe et al. (1969)	[16]
Grilikhes et al. (1975)	[16]
Guerrieri & Talty (1956)	[18]
Kozeki (1973)	[16]
Schrock & Grossman (1962)	[18]
Wongwises & Polsongkram (2006)	[9]
Zhao et al. (2003)	[19]

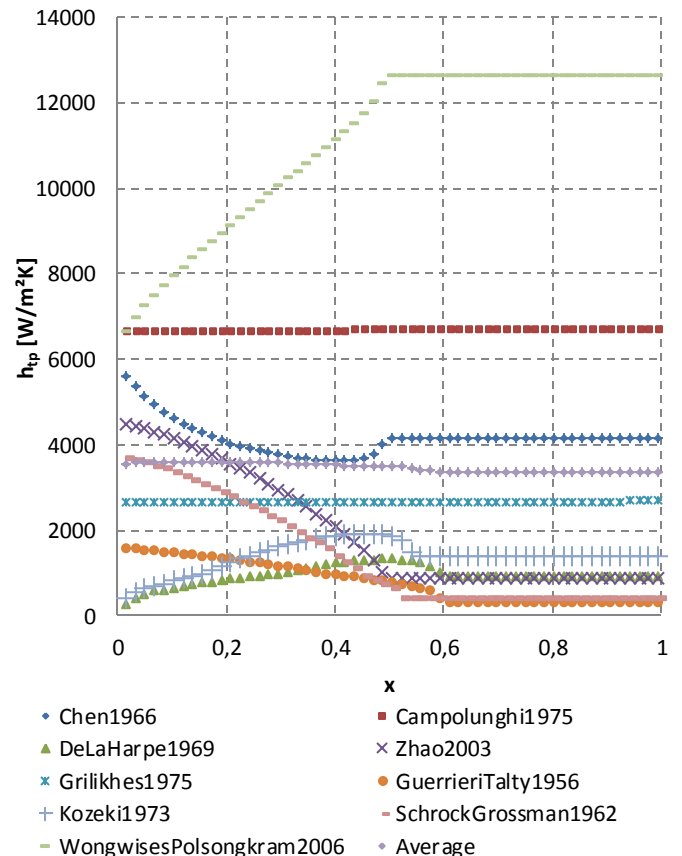
In accordance with the measured input and output temperatures, a linear discretization of both temperature profiles is made. That corresponds to 1000 control volumes. For each control volume, the inlet and outlet temperatures (or enthalpies for the two-phase zone), and the transferred heat are determined. Accordingly, properties of water and R404a are recalculated via CoolProp [20] for each control volume. At each step, the shell side (i.e. hot side) and the tube side (i.e. cold side) convective heat transfer coefficients are calculated. Illustrations of the the control volume analogy is provided in Figure 2.

For the shell side (i.e. hot side) convective heat transfer coefficient, Patil et al. [21] method for helical coil heat exchanger annulus flow is used. For the so-called preheater zone (liquid phase) and the superheated zone (gas phase) of R404a, Patil et al. [21] method for the single-phase flow inside the helical coil is used. After the calculation of overall heat transfer coefficient  $U$ , the required length of each control volume is calculated via  $\epsilon$ -NTU method. At that point it is important to mention that cross-flow configuration (hot side is mixed and cold side is unmixed) is considered for the control volumes. Although the heat transfer direction in the system

resembles a counter-flow configuration, in reality, the control volumes are slightly curved and angled tubes, which makes the cross-flow configuration dominant at discretized level. Moreover, fouling and pressure drops at both sides are neglected.

**Figure 2** Control volume analogy

Figures 3-5 show the local two-phase heat transfer coefficients predicted by the 9 correlations along the whole quality range from 0-100%, for three ORC medium mass flow rates. The average value of convective coefficients of each calculation point is also included in the graph for comparative reasons.

**Figure 3**  $h_{tp}$  vs.  $x$  for  $\dot{m}_c = 0,1$  kg/s and  $T_{sat} = 38,2$  °C

Chen (1966) and Grilikhes (1975) correlations are the closest to the average. Wongwises & Polsongkram correlation (2006) predicts significantly higher values when compared to the rest. There is a 75% deviation among the average  $h_{tp}$  of each correlation.

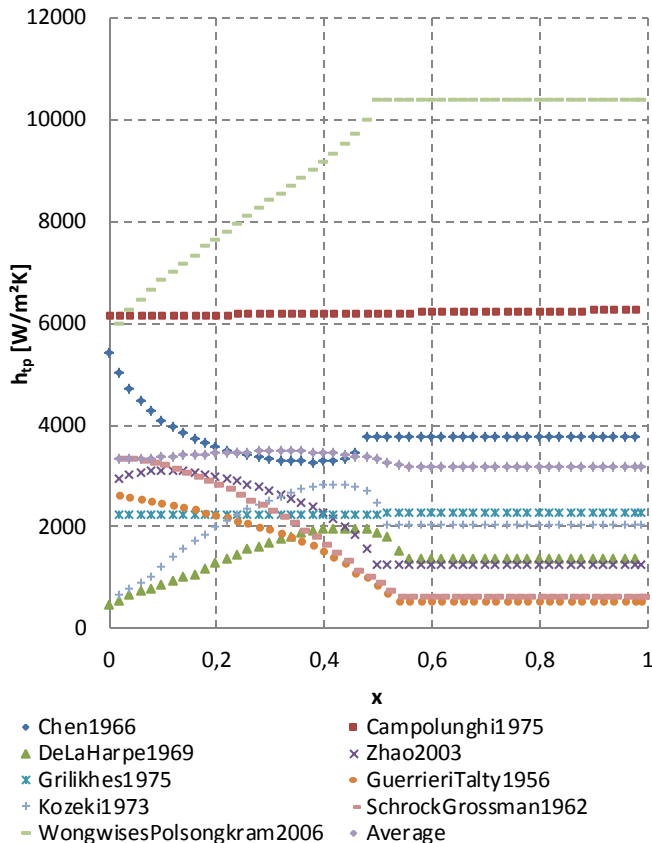


Figure 4  $h_{tp}$  vs.  $x$  for  $\dot{m}_c = 0,17$  kg/s and  $T_{sat} = 50$  °C

Similar to the previous figure, in Figure 4 Wongwises & Polsongkram correlation (2006) predicts significantly higher values in comparison to the rest, yet closer. Alongside the Chen (1966) and Grilikhes correlations (1975), De La Harpe (1969) correlation is close to the average as well. There is 63,83% deviation among the average  $h_{tp}$  of each correlation. Also the  $h_{tp}$  values drop in general.

At Figure 5, at the highest value of the working fluid mass flow rate, the line-up of the predictions change. De La Harpe (1969), Zhao (2003), Kozeki (1973) and Grilikhes (1975) correlations are close to the average value. Wongwises & Polsongkram (2006) correlation predicts the lowest values. The deviation among the average  $h_{tp}$  values from the correlations drop to 42,46%. Also the predicted  $h_{tp}$  values drop observably.

As can be seen from the Figures 3-5, all values tend to stabilize after a vapor quality of approximately 50%. That occurs due to the fact that the Lockhart-Martinelli parameter in the correlations starts to lose its significance in  $h_{tp}$  calculation after that point, as all correlations incorporate the vapor quality into the calculations via that parameter.

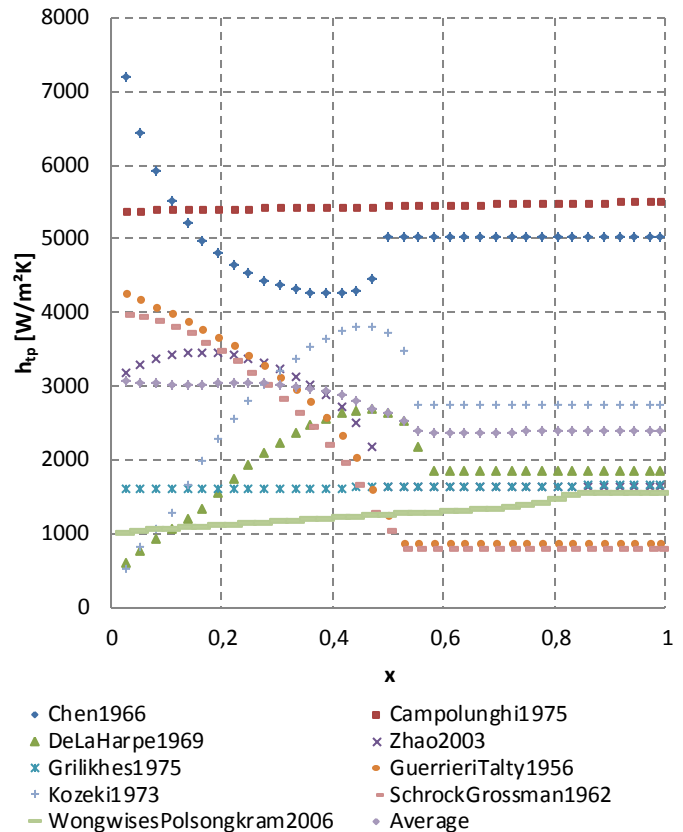


Figure 5  $h_{tp}$  vs.  $x$  for  $\dot{m}_c = 0,24$  kg/s and  $T_{sat} = 64,2$  °C

Furthermore, the prediction capacity of those correlations are assessed by taking the existing helical coil heat exchanger as reference. Only the highest mass flow rate case was taken as reference and investigated, due to the fact that the helical coil is designed for that case. Figure 6 shows the temperature profiles of the shell and the coil side for the case with the highest mass flow rate. The three heat transfer regions are also illustrated.

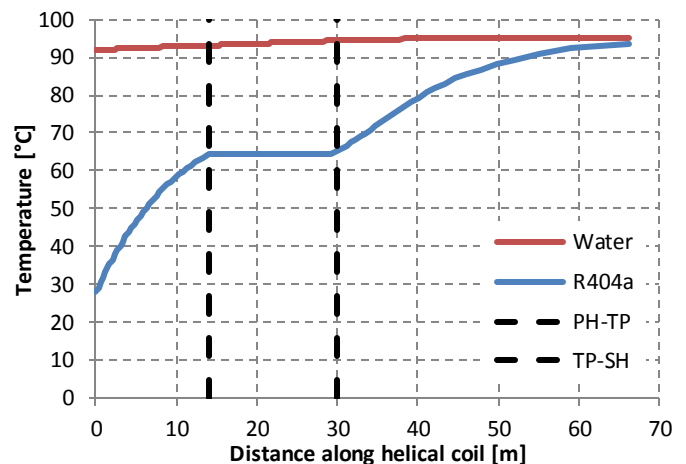


Figure 6 Error margins in total length calculations

Figure 7 shows the calculated helical coil lengths for each correlation and compares them with the existing heat exchanger. A general prediction accuracy of 20% was determined for each correlation to investigate the upper and lower limits of length calculations. The calculations done by incorporating De La Harpe et al. (1969), Grilikhes et al. (1975) and Zhao et al. (2003) correlations are able to predict the existing helical coil length of 66 m within a  $\pm 20\%$  accuracy range. In accordance with the Figure 5, Chen (1966) and Campolunghi et al. (1975) correlations estimate shorter tubes due to higher convective coefficient predictions. The error ranges of the rest of the correlations remain relatively close to the real value. It is important to note that the values shown are the total lengths that incorporate the so-called preheating and superheating zones. Since the single-phase zones are calculated via the same method, the convective coefficients, and thus, the lengths are the same for all correlations. The preheating zone has the length of 13,99 m, while the superheating zone has 35,86 m. The lengths of three zones of the existing helical coil are not included in the analysis since no local temperature measurements are performed.

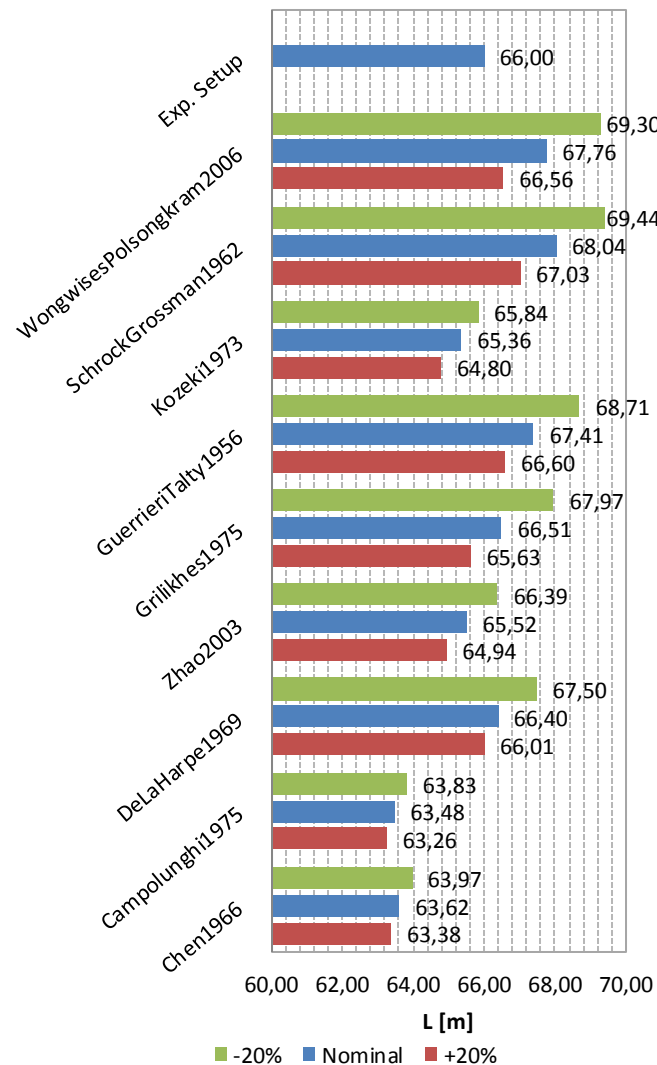


Figure 7 Error margins in total length calculations

Table 4 below shows the average values of calculated two-phase lengths and  $h_{tp}$  for all correlations. Also the deviations among the calculated values are indicated along the changing mass flow rate range, for revealing the dependency of prediction capability on working fluid mass flow rate.

$\dot{m}_c$ [kg/s]	0,1	0,17	0,24
$L_{av}$ [m]	7,08	11,98	16,15
$L_{dev}$	19,44%	13,15%	8,34%
$h_{tp,av}$ [W/m <sup>2</sup> K]	3452	3270	2666
$h_{tp,dev}$	75,00%	63,83%	42,46%

By taking all correlations in consideration, the average two-phase coil lengths and average two-phase heat transfer coefficients, as well as the mean absolute deviations of the calculated values from each correlation is given with respect to the increasing mass flow rate. As the mass flux increases, the  $h_{tp}$  decrease and thus the calculated length increases. Moreover, the calculated length is more influenced than the  $h_{tp}$ . This might seem in contradiction with the fact that the in-tube convective coefficients are higher in comparison to the shell side (i.e. the overall heat transfer is shell side dominated), and  $h_{tp}$  should have a relatively weak effect on the calculated length. However, this phenomenon occurs since the higher mass flow rate measurements are made at higher saturation temperatures, which lead to less temperature difference between the hot and the cold side during evaporation. That leads to a lower heat transfer performance. On the other hand, deviations decrease with the increasing mass flow rate. That implies the fact that the choice of two-phase correlation matters less when at higher mass flow rates. In other words, research for more accurate prediction methods may be necessary for low mass flow rates.

## CONCLUSION

The following conclusions are made from the present study related to flow boiling in a helical coil heat exchanger being used in a solar ORC system:

- The two-phase heat transfer correlations for helical coils predict significantly different values,
- With an assumed error range of  $\pm 20\%$  Zhao et al. (2003), Grilikhes (1975) and De La Harpe et al. (1969) correlations predict the existing heat exchanger most accurately,
- Chen (1966) and Campolunghi (1975) correlations significantly overpredict the  $h_{tp}$ ,
- The deviations among the predictions become less as the mass flow rate increases
- Experimental research is necessary especially for low mass flow rates for deducing accurate correlations, whereas at higher mass flow rates the error caused by the deviations between correlations remain in an acceptable range ( $<10\%$ ). In other words, experimental research for higher mass flow rates is of less importance.

## REFERENCES

- [1] Chen, H., Goswami, D. Y. and Stefanakos, E. K., A review of thermodynamic cycles and working fluids for the conversion of low-

- grade heat, *Renewable and sustainable energy reviews*, Vol. 14(9), 2010, pp. 3059-3067
- [2] Bao, J. and Zhao, L., A review of working fluid and expander selections for organic Rankine cycle, *Renewable and Sustainable Energy Reviews*, Vol. 24, 2013, pp. 325-342
- [3] Quoilin, S., Van Den Broek, M., Declaye, S., Dewallef, P. and Lemort, V., Techno-economic survey of Organic Rankine Cycle (ORC) systems, *Renewable and Sustainable Energy Reviews*, Vol. 22, 2013, pp. 168-186
- [4] Walraven, D., Laenen, B. and D'haeseleer, W., Comparison of shell-and-tube with plate heat exchangers for the use in low-temperature organic Rankine cycles. *Energy Conversion and Management*, Vol. 87, 2014, pp. 227-237
- [5] Kaya, A., Lazova, M. and De Paepe, M., Design sensitivity analysis of using various in-tube condensation correlations for an air-cooled condenser for ORCs, *11th International Conference on Heat Transfer, Fluid Mechanics and Thermodynamics (HEFAT)*, 2015, pp. 594-599
- [6] Kaya, A., Lazova, M. and De Paepe, M., Design and rating of an evaporator for waste heat recovery organic rankine cycles using SES36. In *3rd International Seminar on ORC Power Systems (ASME ORC 2015)*, 2015, pp. 402-411
- [7] Lecompte, S., Lemmens, S., Huisseune, H., van den Broek, M. and De Paepe, M., Multi-Objective Thermo-Economic Optimization Strategy for ORCs Applied to Subcritical and Transcritical Cycles for Waste Heat Recovery, *Energies*, Vol. 8(4), 2015, pp. 2714-2741
- [8] van den Broek, M., Quoilin, S., Declaye, S., Lemort, V. and de Goedelaan, G.K., Organic Rankine Cycle Systems: A Techno-Economic Overview, In *European Metallurgical Conference 2013*, Vol. 2, 2013, pp. 833-844, GDMB Verlag GmbH
- [9] Wongwises, S. and Polsongkram, M., Evaporation heat transfer and pressure drop of HFC-134a in a helically coiled concentric tube-in-tube heat exchanger, *International Journal of Heat and Mass Transfer*, Vol. 49(3), 2006, pp. 658-670
- [10] Quoilin, S., Orosz, M., Hemond, H. and Lemort, V., Performance and design optimization of a low-cost solar organic Rankine cycle for remote power generation. *Solar Energy*, Vol. 85(5), 2011, pp. 955-966.
- [11] Orosz, M.S., Mueller, A., Quoilin, S. and Hemond, H., Small scale solar ORC system for distributed power. *MIT Research Report*, 2009, Cambridge: MA USA.
- [12] Ferrara, F., Gimelli, A. and Luongo, A., Small-scale concentrated solar power (CSP) plant: ORCs comparison for different organic fluids. *Energy Procedia*, Vol. 45, 2014, pp. 217-226
- [13] Lazova, M., Daenens, D., Kaya, A., Van Belleghem, M., Huisseune, H., Kosmadakis, G., Manolakos, D. and De Paepe, M., Design of a supercritical heat exchanger for an integrated CPV/T-Rankine cycle, In *3rd International Seminar on ORC Power Systems (ASME ORC 2015)*, 2015, pp. 412-421
- [14] Klein S.A., Engineering equation solver (EES), academic professional version, F-chart software (2015)
- [15] Kosmadakis, G., Manolakos, D. and Papadakis, G., Experimental investigation of a low-temperature organic Rankine cycle (ORC) engine under variable heat input operating at both subcritical and supercritical conditions, *Applied Thermal Engineering*, Vol.92, 2016, pp. 1-7
- [16] Jensen, M.K., Boiling heat transfer and critical heat flux in helical coils, *Retrospective Theses and Dissertations*, 1980, Paper 7336
- [17] Chen, J.C., Correlation for boiling heat transfer to saturated fluids in convective flow, *Industrial & engineering chemistry process design and development*, Vol. 5(3), 1966, pp. 322-329
- [18] Nariai, H., Kobayashi, M. and MATSUOKA, T., Friction Pressure Drop and Heat Transfer Coefficient of Two-Phase Flow in Helically Coiled Tube Once-Through Steam Generator for Integrated Type Marine Water Reactor, *Journal of Nuclear Science and Technology*, Vol. 19 (11), 1982
- [19] Zhao, L., Guo, L., Bai, B., Hou, Y. and Zhang, X., Convective boiling heat transfer and two-phase flow characteristics inside a small horizontal helically coiled tubing once-through steam generator, *International journal of heat and mass transfer*, Vol. 46(25), 2003, pp. 4779-4788
- [20] Bell, I.H., Wronski, J., Quoilin, S. and Lemort, V., Pure and Pseudo-pure Fluid Thermophysical Property Evaluation and the Open-Source Thermophysical Property Library CoolProp, *Industrial & Engineering Chemistry Research*, Vol. 53 (6), 2014, pp. 2498 - 2508
- [21] Patil, R.K., Shende, B.W. and Ghosh, P.K., Designing a helical-coil heat exchanger, *Chemical Engineering*, Vol. 92(24), 1982, pp. 85-88